Thesis/
Reports
Gutierez-
Tiera,
B. S.

THESIS / REPORTS
GUTIERREZ-TEIRA
In REVIEW

03-JV-11222014-157
Final Report
Part 1

FKK127

Using satellite imagery and hemispherical photography to map the effects of vegetation cover on solar radiation and stream temperatures at a basin scale.

Bárbara Gutiérrez-Teira[1], Charles H. Luce, David Nagel, and Jason B. Dunham[2]

Rocky Mountain Research Station, Boise Aquatic Sciences Lab, 322 E. Front St., Suite 401, Boise, ID 83702.

Corresponding Author:
Luce, Charles H.
cluce@fs.fed.us
Rocky Mountain Research Station,
Boise Aquatic Sciences Lab,
322 E. Front St., Suite 401
Boise, ID 83702.
Ph: (208) 373-4382
Fax: (208) 373-4391

1. Now at
Universidad Europea Miguel Cervantes
Valladolid, 47012
Spain
bargute@yahoo.es

2. Now at
U.S. Geological Survey, Forest And Rangeland Ecosystem Science Center
3200 SW Jefferson Way
Corvallis, OR 97331
jdunham@usgs.gov

ABSTRACT

Water temperature is a key physical property in stream ecosystems because of its effect upon organisms. Accordingly, it is an important criterion for regulation of land management activities. Solar radiation is the dominant factor controlling stream temperatures, and the amount of solar radiation reaching a stream is controlled by basin topography and riparian vegetation. Alterations in riparian vegetation by anthropogenic or natural disturbances may alter stream temperature. Consequently, evaluating or modeling stream temperature patterns over river basins requires estimates of shade for extensive areas. It is generally not feasible to collect such information from the ground, and methods are needed to estimate shade from remotely sensed data. In this paper we use hemispherical photography and satellite imagery supported by field measurements to analyze the relationships between shade values in specific stream reaches and the water temperatures in those streams. Shade is evaluated through estimates of solar radiation, obtained using hemispherical canopy photography. Water temperature was measured in the field in more than 10 streams during two summers. Streams with three disturbance levels: unburned, burned, and burned and disturbed, were selected for study. The vegetation characteristics (type of vegetation and disturbance level) of each site were recorded *in situ*. Riparian vegetation was mapped using Landsat Thematic Mapper imagery, which allowed us to estimate radiation values along the stream channel. Relationships were obtained among radiation values, disturbance level, and water temperature. The positive results obtained suggest the possibility of mapping stream temperatures at a basin scale.

Keywords: satellite imagery, hemispherical photography, temperature, radiation, streams, vegetation, disturbance

INTRODUCTION

Solar radiation is a major energy source for aquatic systems, and has been established as a dominant factor controlling stream temperatures (Sinokrot and Stefan, 1993; Webb and Zhang, 1997, 1999; Johnson, 2004). The riparian zone and the shade it provides are the main factors regulating the amount of solar radiation that enters a stream, thus controlling water temperatures (Gray and Edington, 1969, Johnson and Jones, 2000; Johnson, 2004; Danehy et al, 2005), especially in narrow streams (Rutherford et al. 1997). Canopy architecture influences solar radiation interception and transmittance according to variations in space and time. The physical structure of the riparian zone naturally changes along the continuum from headwaters to river mouth (Vannote *et al.*, 1980, Poole and Berman, 2001). Thus, the size and location of canopy gaps, the angle of solar incidence, stream width, and the tree species and sizes found along the banks (Hardy *et al.*, 2004) are important factors altering the radiation reaching the stream. For example, coniferous and deciduous trees can provide significant amounts of shade because of their heights and extensive canopies, whereas in relatively open valley systems, a combination of different shrubs can provide lesser but important amounts of shade (Beschta, 1997).

Fire, insects, disease, wind damage, and forest management are the key mechanisms reducing riparian canopies, and in order to evaluate tradeoffs between alternative management scenarios, including how those scenarios affect natural

disturbances, there is a need to predict stream temperatures. Several models have been developed to accomplish this task (see Sinokrot and Stefan, 1993; Sugimoto *et al.*, 1997), however many of them require an intensive description of the site's environmental conditions, which in many cases represents a substantial financial, technical and logistical burden. It would, therefore, be valuable to develop efficient methods that will allow managers to estimate riparian shade and stream thermal characteristics across a basin.

Hemispherical photography is one of the best accepted methods to estimate solar radiation from the ground (see Weiss *et al.*, 1991; Robinson and McCarthy, 1999). Attempts to evaluate or model stream shade patterns over river basins with this methodology alone, however, would require measurements over extensive stream lengths, which is impractical, particularly in light of the need to take photographs near sunrise or sunset. Measurements of crown cover or basal stem area per unit land area, which are not sensitive to the time of day they are made, may provide an alternative. Such proxies would also be valuable because they can be linked directly to silvicultural prescriptions and easier regulation of forest practices. They would still pose significant monitoring costs for large basins.

The use of satellite imagery may be a more practical approach to provide such estimates. It has proven to be a useful tool for characterizing large spatial extents for many applications (see Malingreau, 1986; Hutchinson, 1991) and it provides a cost-effective way to inventory large areas with consistent information (Congalton *et al.*, 1993, 2002; Bauer *et al.*, 1994; Wolter *et al.*, 1995). One of the most common practices to assess vegetation characteristics with satellite imagery is the use of vegetation indices obtained as a

combination of remote sensing bands, since the value of the index may be related to the amount of vegetation in every pixel of the image. One of the most common indices used is the NDVI, that is, the Normalized Difference Vegetation Index (Kriegler et al. 1969; Rouse et al., 1973). Many authors have found NDVI to be related with certain vegetation cover characteristics such as the leaf area index (LAI) or the crown closure (e.g. White *et al.*, 1997, Lawrence and Ripple, 1998, Xu *et al.*, 2003). Most tools using NDVI, however rely on relatively homogeneous plant types. Complex assemblages of plant types (e.g. mixed conifers and broadleaf shrubs) require different tools, such as classification (Huguenin *et al.*, 1997).

Remote sensing has been effective for classifying forest vegetation covers for large areas (e.g. Williamson, 1994; Huguenin *et al.*, 1997), and specifically, it has been used to map riparian classes associated with rivers, lakes and wetlands with high accuracy (e.g. > 80 %; Hewitt, 1990, Narumalani *et al.*, 1997). Our purpose in this study was to evaluate the utility of remote sensing, either through band ratios or classification for estimating transmittance of solar radiation along a stream. We used hemispherical photography as the basis for developing the model, and validated the results using observed vegetation types and stream temperatures.

METHODS

Overview

We collected hemispherical photography at 181 sites along with vegetation stand information. These data were used with remote sensing data to develop an estimate of solar radiation. Two methods were attempted. In the first, we correlated NDVI to shade

measurements, and in the second we classified the vegetation and looked at how well that classification predicted differences in shade. We validated the classification method for estimating shade by comparing the remotely sensed estimate of radiation to degree of disturbance on streams that had recently burned or experienced debris flows. We further validated the approach by essentially treating the stream temperature as an indicator of incoming solar radiation and correlating estimated radiation along a stream against stream temperatures, which also served to demonstrate the potential utility of remote sensing for broad scale estimation of stream temperature.

Study Site

The study was conducted in the Boise River basin in southwest Idaho (Figure 1). The Boise River basin is in the southern part of the Idaho batholith, an area noted for its highly erodible granite rock and steep topography. Precipitation ranges from 600-1000 mm per year, with greater amounts at higher elevations. Most precipitation falls in the winter as snow with rare winter or spring storms that deliver warm rain-on-snow events that can lead to flooding. The basin has cold, wet winters with freezing temperatures contrasting with generally hot and dry summers with air temperatures commonly exceeding 30°C.

Riparian tree and shrub species consist primarily of willow (*Salix*, spp.), Black cottonwood (*Populus trichocarpa*), alder (*Alnus*, spp.), Engelmann Spruce (*Picea engelmannii*), Lodgepole pine (*Pinus contorta*), Ponderosa Pine (*Pinus ponderosa*), Douglas-fir (*Pseudotsuga menziesii*), and several true firs (*Abies* spp.). Hillslope vegetation within study streams consisted of mixed conifer, Ponderosa pine forest, and

shrubsteppe. These vegetation types are characterized by mixed severity fires with return intervals ranging up to 34 years (Morgan et al., 1996, Brown and Smith 2000).

The area has experienced several major fires in the last fifteen years resulting in approximately 40% of the basin in a burned condition. Several streams with severe burns also experienced debris flows. The extensive burning over such a large area and the associated geomorphic events have opened opportunities for research to examine the effects of fire on streams and stream ecosystems, and many researchers have worked in the area providing a rich description of physical and ecological processes in streams (e.g. Istanbulluoglu et al., 2002, 2003, 2004, Benda et al., 2003, Meyer and Pierce, 2003, Miller et al., 2003, Dunham et al., 2006)

Hemispherical Photography and Stand Data

Hemispherical canopy photography is a technique used to measure daily and monthly changes over time in forest light environments (Rich *et al.*, 1993) by means of upward looking photographs taken with a viewing angle of 180°. Photos were acquired in June, 2003 just before dawn and just after sunset, during fading light conditions, to avoid overexposure of the film. Approximately five photos were acquired at each of forty-four field sites (Figure 2); of these we were able to analyze 181. The photos were spaced about 50 meters apart along the stream at the center of the stream, 1 meter above the water surface. The locations were distributed among different vegetation cover types and stream size. Stream bankfull width averaged 1 – 8 meters. Photos were processed using

Hemiview software (Dynamax Inc.[1]). Total solar radiation (direct plus diffuse) for June was computed for each photo location.

An average radiation value was then computed for three different common riparian vegetation types found in the watershed: open in character (little or no canopy), deciduous shrub, and conifer. This value represents the total amount of solar radiation that is able to pass through the canopy to the stream surface. To determine an average radiation value for each vegetation class, the canopy photos were divided into the three respective categories and the mean total solar radiation was computed for each. In the remote sensing section to follow, satellite imagery will be classified into these same three vegetation classes to estimate incoming solar radiation along the stream channel.

At the same sites, the basal area, which is the cross sectional area of wood per unit area of ground, of the standing wood vegetation greater than six inches in diameter was measured using a BAF 20 prism (Dilworth, 1981). Basal area has been correlated with vegetation biomass, which presumably has some relationship to the amount of shade below a stand. Measurements were taken from the photo point around 360°, identifying the tree species and stem diameter. Radiation obtained with hemispherical photos was regressed against basal area. In addition, two horizontal photos were taken at each sample site using a standard digital camera to record the dominant vegetation type.

Stream Temperature Data

During July-September 2002, temperature loggers (Onset Tidbits) were placed in fourteen streams of the watershed (Figure 3) with ten loggers in each stream, except two

[1] The use of trade or firm names is for reader information only and does not constitute endorsement by the U.S. Government.

that had nine, making a total of 138. During June-September 2003, 10 more loggers were placed in ten streams of the watershed (Figure 4) for a total of 100. Loggers were set inside PVC cases to protect them from direct solar radiation and collected temperatures every 30 minutes (Dunham et al. 2005).

Each of the streams was classified using aerial photography and field observation into three disturbance classes: unburned, burned, and burned with debris flow scour (Dunham et al., 2006). Unburned sites had the original, primarily coniferous, vegetation. Burned sites had experienced severe stand replacing fire, leaving conifers dead. Sites that had burned and experienced debris flows, a massive landslide-like movement of mud, boulders, and logs through the channel, saw reductions in shrub vegetation as well. Dunham et al., (2006) referred to this latter class as "burned and reorganized."

Daily average and maximum temperatures were calculated at each site to obtain the Maximum Weekly Average Maximum Temperature (MWMT) and the Maximum Value of Average Weekly Temperature (MWAT). MWMT is the highest maximum temperature summarized over a continuous seven-day period, and MWAT is the highest average temperature summarized over each day of a continuous seven-day period. With these values, we calculated the average MWMT and the average MWAT for every stream each year. Data were analyzed for the period July 1 to September 15 for each year. In 2002, this missed the actual peak stream temperatures, which were reached in late June, however a secondary peak in August is represented in this analysis.

Remote Sensing Data

We analyzed Landsat 7 ETM+ satellite imagery of the basin, acquired on July 10, 2002. Standard image processing techniques were used to prepare the data for classification. The imagery was geo-rectified and terrain corrected to a spatial resolution of 30 meters. Digital Orthophoto Quads (DOQ) with two meter spatial resolution and United States Geological Survey (USGS), National Elevation Dataset (NED) data were utilized for ground control and terrain correction, respectively. The cubic convolution algorithm was used to resample the data and a root mean square error of approximately 15 meters was obtained. This error indicates that the overall spatial accuracy of the output image was within one half of the resultant cell size, being 30 meters. Next a topographic normalization routine was applied to the image to remove differential illumination, which was caused by the rugged terrain in our study area. We used a standard Lambertian reflection model (Smith, et. al., 1980) to normalize illumination along the valley bottom slopes where our analysis was conducted.

The NDVI index was calculated from the red and near infrared bands (3 and 4). This index, which uses a combination of the visible and near infrared wavelengths has a value between -1 and 1 and is calculated through the following equation:

$$NDVI = (NIR - red)/(NIR + red) \quad 1$$

We regressed the radiation from the hemispherical photos against the NDVI values obtained for the pixel at each point.

In a separate procedure, the pre-processed satellite image was classified into three vegetation classes: open, broadleaf shrub, and conifer. Open represented areas where

canopy cover was less than 10%; the broadleaf shrub category was used where willow shrubs predominated, and conifer was classified when ponderosa pine, Douglas-fir, or subalpine fir dominated the overstory. A standard maximum likelihood algorithm was used to classify the imagery and the result was refined using an ISODATA clustering technique (Jensen, 1996). The horizontal photos and DOQ data were used to select the training sites that were necessary as input to the maximum likelihood program. Analysis of Variance (ANOVA) was computed to test differences of radiation among the three cover types.

In order to extract vegetation information and hence incident radiation along the stream channels, digital stream line data were required for the study area. We chose to generate "synthetic" stream lines from the NED elevation data because this representation of stream channels spatially matched the satellite imagery, which had been geo-rectified using the same elevation data. We used a software suite called TAUDEM to generate the lines, which resulted in a stream network that closely matched the blue lines found on the USGS 1:24,000 scale topographic map series (Tarboton, 1997). The stream lines were overlain with the classified vegetation data using a Geographic Information System (GIS) and the vegetation information was extracted along the riparian corridor. This process resulted in a single line of pixels along the stream channel representing vegetation and thus incident radiation.

Temperature logger point locations, recorded using a GPS receiver, were snapped to the TAUDEM stream lines. To analyze the relationship between radiation and disturbance, GIS was used to extract incident radiation information 1 km upstream from

each temperature logger location in order to generate average radiation values. The vector stream lines 1 km upstream from each logger were overlain with the raster classification and the coincident vegetation data were extracted. Once the vegetation data were extracted along the riparian corridor, an average upstream radiation value was computed for each temperature logger. From this information we were able to evaluate the relationship between the estimated average radiation and the three observed disturbance classes and their average temperatures.

We also extracted vegetation data 2 km upstream from each temperature logger, this time including tributaries, so that radiation affecting all of the water bodies above the logger was taken into account when analyzing its effects upon temperature. Average radiation for each stream was calculated for each of the two years. The results were plotted against the observed temperatures and regression models were built to observe the dependence of water temperature (MWMT and MWAT) on radiation (R). Radiation data were also summarized at 1, 3, 4, and 5 km upstream from each temperature logger with tributaries, however these data were not used because the 2 km length yielded the best correlation.

RESULTS

Radiation versus Basal Area

Clear sky radiation values estimated from the hemispherical photos averaged during the month of June ranged from 118 to 1038 $MJ/m^2/yr$. A weak relationship existed between the basal area measured at the site and solar radiation (Figure 5; $F(1,167)=45.50$,

$p<0.0001$, $R^2=0.21$). In the plot we also see a greater variability for low stand basal areas compared to high.

Radiation versus NDVI

Although statistically significant, the relationship between remotely sensed NDVI and radiation was relatively uninformative (Figure 6; $F(1,188)=9.81$, $p=0.002$, $R^2=0.05$).

Radiation versus Classified Vegetation and Observed Disturbances

Vegetation classification was correct in 75% of the points where we had vegetation observations; 6% were classified with greater radiation than observed, and 19% were classified as having less radiation. Most of the misclassification was either Grass or Shrub being classified as conifer, a clear bias towards classification as conifer. Note that there are uncertainties in observed classification, registration of sites to pixels, and uncertainties in the reflectance based classification behind these patterns.

Conceptually, using the vegetation classification approach should result in less precision in estimates at a particular pixel than a regression might, however based on a simple classification into open conditions, shrub, and conifer, a strong discernment between sites was possible. The mean radiation values in June, derived from the canopy photos, for the open, shrub and conifer classes respectively were 795, 663, and 531 $MJ/m^2/yr$, respectively, reflecting the general expected trend of decreasing radiation with increasing vegetation (Figure 7; $F(2,178)=25.54$, $p<0.0001$). The fraction of the variance explained by this rough classification of vegetation ($R^2=0.22$) is comparable to that from knowing the stand basal area ($R^2=0.21$).

The distribution of vegetation types within the three disturbance classes, unburned, burned, and burned with debris flow, reflects the nature of the disturbances (Figure 8). Unburned streams were primarily conifer covered. Burned sites lost much of their conifer component to the severe fire, but saw substantial increases in representation of shrub and grass cover. Sites experiencing both severe fire and a debris flow saw a more complete loss of conifer cover, because of the continuous nature of the debris flow event. These sites also saw an increase in proportion of segments classified as grass. These image derived estimates of cover matched qualitative observations and photographs of the streams showing the same general pattern. The average radiation estimated along the streams of these three types using the classification reflects the disturbance class (Figure 9; $F(2,14)=9.8$, $p=0.002$, $R^2=0.58$).

Validation against observed temperatures

The stream averaged values of MWAT for the 14 streams measured in 2002 ranged from 8.80 °C for the coldest stream to 19.69 °C for the warmest. In the ten streams measured in 2003 the range was 9.92 °C to 17.07 °C (Table 2).

MWAT and MWMT were significantly related to the disturbance classification of the streams in both 2002 and 2003 (Figure 10, Table 3). At a simple classification level, if the estimated radiation values can successfully distinguish between disturbance levels, that knowledge is sufficient for estimating gross differences in temperature.

Relationships between the stream average radiation and stream average MWMT and stream average MWAT for 2002 and 2003 are shown in Figure 11. The equations for the linear regressions are compiled in Table 4. In year 2002, the relationships had an R^2

85% and 86% for MWAT and MWMT, respectively, whereas in 2003 the R^2 decreased to 51% and 54%. This decrease in the R^2 is in part caused by the gap in data for stream-average radiation values between 550 and 650 MJ/m^2/yr giving the point with a radiation of 515 MJ/m^2/yr with a comparatively warm temperature great leverage in the regression. That stream was added for the 2003 data set; it was longer and had a greater contributing area than all but one other stream, which is probably part of why it was warmer. Removing that stream from the regression would increase the R^2 to 68% for either MWAT or MWMT.

DISCUSSION

The basic question at hand is "can we reliably estimate solar radiation inputs to streams based on remote sensing data?" We ask this because ground based estimates are expensive and difficult to gather, particularly when considering estimates of stream temperature across a basin. Hemispherical photography, for example can only be captured during sunrise and sunset, or on overcast days.

To investigate this question, we used estimates of radiation derived from hemispherical photographs as a key regression and calibration variable, we further validated remote sensing based estimates against field observations of the condition and measurements of stream temperature. These latter two validation approaches integrate over space reducing issues associated with registration of point data with imagery.

Initially we compared radiation with ground-based measurements of canopy biomass to avoid registration errors associated with remote sensing. This conceptually provides some expectation for performance of remote sensing based analyses, because

remote sensing has commonly been used to estimate leaf area or canopy biomass. Specifically, we measured the stem basal area which has been correlated to canopy biomass and leaf area. By measuring the stem basal area at the same location as the hemispherical photograph, we avoid errors associated with registration to give us an estimate of the amount of information contained in estimates of leaf area or biomass. Figure 5 shows a significant and linear relationship; however the low R^2 of 0.21 initially suggests that we should not expect a great deal of information.

An interesting characteristic of the plot, though, reveals that some of the scatter may be due to a mismatch in the scale of the sampling. While the measurement of basal area has a support scale (footprint) on the order of several canopy diameters, the hemispherical photograph integrates only a few meters. Most of the information about variation in radiation in a hemispherical photograph is in a small circle slightly south of the center of the photograph. Assuming that most of the information is within 15 degrees of the center, the photograph would have essentially a 5-m support scale in a 20-m tall forest. In the same forest, the basal area measurement could realistically have a footprint of 40-m. The camera then is taking a 5-m diameter picture out of a 40-m diameter stand. What this scale mismatch means is that in broken canopy, sometimes the camera is under a branch, and sometimes it is not. We expect the camera to more consistently be under branches in stands with high canopy cover, which is reflected in less scatter at the highest basal areas. This suggests that radiation estimates from multiple camera settings several meters apart may be more informative for comparison to measurements with large footprints, e.g. stand density, basal area, or remote sensing pixels.

A second very simple analysis was to look at the utility of NDVI to estimate radiation. Although the use of satellite band ratios and indices has been a useful tool to estimate LAI or crown closure in different landscapes (see Wiegand *et al.*, 1992, White *et al.*, 1997, Xu *et al.*, 2003), we found no relationship between the NDVI index and the radiation values obtained in the field (Figure 6). Primarily, we expect that this is because such methods require monospecific vegetation cover. In heterogeneous forests and riparian areas, classification techniques are expected to fare better (Huguenin, et al., 1997). The scale mismatch may also be a factor here as well, but because there is substantially less information in NDVI than the stand basal area, the heterogeneity of the vegetation is probably a more important factor.

In contrast, vegetation classification, even using a very simple set of life form classes was fairly informative. With an R^2 of 0.22 it was as informative as knowing the stand basal area from ground measurements, and substantially less expensive and time consuming to collect. The relationships derived from the classified imagery agree with those found in other studies between radiation and vegetation cover (Breshears *et al.*, 1997; Canham and Burbank, 1994), disturbance (Beschta and Taylor, 1988; Hatten and Conrad, 1995), or species (Beschta, 1997). That is, radiation increases with disturbance level and it is affected by the vegetation type.

Inherent in these point scale relationships are both scale-mismatch sampling errors and registration errors, limiting the expectations for the amount of variance explained; so we investigated validations averaging along reaches. In the several reaches classified according to their degree of disturbance we see a pattern in the proportion of pixels

classified as conifer, shrub, or grass (Figure 8). The fact that the debris-flow scoured streams showed mostly grass pixels reflected the lack of shrub resprouting that had occurred on these reaches in the decades since the events, a characteristic noted in the field. This pattern of relative proportions of pixels in each class yielded the expected pattern of increased radiation as a function of degree of disturbance (Figure 9). This estimate of increase temperature as a function of disturbance is validated by the pattern of increased temperature as a function of disturbance (Figure 10).

Comparison of radiation estimated from classification to stream temperatures demonstrates the utility of the approach, even with the simple classification used here. An ability to map solar radiation and the relationship between solar radiation and stream temperature may provide new opportunities to improve large scale estimation and mapping of stream temperatures. While latitude and elevation are widely regarded as major controls on stream temperature (e.g. Keleher and Rahel, 1996, Dunham et al., 1999), such regressions are approximate and see substantial noise for smaller streams (e.g., Dunham et al. 2003). While air temperature is a useful surrogate at spatial scales of millions of square kilometers, other influences become important at smaller scales. Because solar radiation has a major influence on stream temperature, remote sensing may provide a tool that can be used for analyses of stream temperature patterns in basins on the order of tens to tens of thousands of square kilometers, in the class of "intermediate" scale basins where data needs are critical (*sensu* Fausch et al., 2002). Furthermore, such a tool may provide an important model parameter for distributed physically based modeling of stream temperature.

This study used data from several sources in order to build a strong case. As is common, however, some of the ability to meld multiple separately designed studies is fortuitous, and seldom provides the strongest testing, validation, or statistical power for building predictive relationships. While the rudimentary relationships described herein suggest promise for future development, researchers doing such development would be assisted by knowing a few things. The point scale ground sampling versus pixel scale satellite observation issue has been discussed in detail already. It is important to realize that multiple closely grouped hemispherical photographs do not represent several independent observations, but are used to reduce the variability among the independent samples each comprising groups of points. Similarly, stream temperature reflects a sum (or average) of radiant energy inputs downstream, and there can be a great deal of spatial autocorrelation along a given stream, so that individual measurements within a given stream may not represent independent samples. Sampling across multiple streams will increase the statistical power. Improvements in classification techniques and estimating shade based on multiple variables, e.g. vegetation classification, stream width, and orientation, may also provide better results. Finally researchers should recognize that solar radiation is only one, albeit a major, component of the stream energy balance, and that other stream characteristics controlling stream temperature such as the degree of hyporheic exchange (e.g. Moore et al. 2005) or groundwater inflow will necessarily degrade the relationship between averaged radiation and stream temperature.

CONCLUSIONS

The joint use of satellite imagery and hemispherical photographs can be a useful tool to classify different vegetation areas and estimate their radiation transmission, making possible the analysis of extensive areas in a relatively fast and reliable way. With this methodology we derived a relationship between remotely sensed riparian vegetation classification and transmitted solar radiation. We demonstrated that this relationship accurately discerns levels of disturbance associated with wildfire and post-fire debris flows, and, further, that the estimated radiation correlates to stream temperature. These results reaffirm the importance of stream vegetation in controlling the amount of solar radiation reaching the waters of small streams, and suggest that remote sensing of riparian canopy could be useful for large scale stream temperature prediction.

REFERENCES

Bartholow, J. M. 2000. Estimating cumulative effects of clearcutting in stream temperatures. Rivers **7**(4): 284-297.

Bauer, M., Burk, T., Ek, A., Coppin, P., Lime, S., Walsh, T., Walters, D., Befort, W. and Heinzen, F. 1994. Satellite inventory of Minnesota forest resources. Photogrammetric Engineering and Remote Sensing **60**(3): 287-298.

Beschta, R. L. 1997. Riparian shade and Stream Temperature: An alternative perspective. Rangelands **19**(2): 25-28.

Beschta, R. L. and Taylor, R. L. 1988. Stream temperature increases and land use in a forested Oregon watershed. Water Resources Bulletin **24**(1): 19-25.

Breshears, D. D., Rich, P. M., Barnes, F. J. and Campbell, K. 1997. Overstory-Imposed heterogeneity in solar radiation and soil moisture in a semiarid woodland. Ecological Applications **7**(4): 1201-1215.

Brown, G. W. and Krygier, J. T. 1970. Effects of clear-cutting on stream temperatures. Water Resources Research **6**(4): 1133-1139.

Brown, J.K.; Smith, J.K., eds. 2000. Wildland fire in ecosystems: effects of fire on flora. Gen. Tech. Rep. RMRS-42-vol. 2. Ogden, UT: U.S. Department of Agriculture Forest Service, Rocky Mountain Research Station.

Canham. C. D. and Burbank, D. H. 1994. Causes and consequences of resource heterogeneity in forests: interspecific variation in light transmission by canopy trees. Canadian Journal of Forest Research **24**: 337-349.

Congalton R., Green, K., Teply, J. 1993. Mapping old growth forests on National forest and park lands in the Pacific Northwest from remotely sensed data GeoInfo Systems **3**(2): 31-41.

Congalton R. G., Birch, K., Jones, R. and Scriever, J. 2002. Evaluating remotely sensed techniques for mapping riparian vegetation. Computers and Electronics in Agriculture **37**: 113-126. DOI:10.1016/S0168-1699(02)00108-4.

Danehy, R. J., Colson, C. G., Parrett, K. B. and Duke, S. D. 2005. Patterns and sources of thermal heterogeneity in small mountain streams within a forested setting. Forest Ecology and Management **208**:287-302. DOI:10.1016/j.foreco.2004.12.006

Dilworth, J. R. 1981. Log Scaling and Timber Cruising. Oregon State University Book Stores, Inc. Corvallis, Oregon.

Dunham, J., G. Chandler, B. Rieman, and D. Martin. 2005. Measuring stream temperature with digital data loggers: A user's guide. General Technical Report. RMRSGTR-150WWW. Fort Collins, CO: U.S. Department of Agriculture, Forest Service, Rocky Mountain Research Station. 15pp.

Dunham, J.B., M.M. Peacock, B.E. Rieman, R.E. Schroeter, and G.L. Vinyard. 1999. Local and geographic variability in the distribution of stream-living Lahontan cutthroat trout. Transactions of the American Fisheries Society 128:875-889.

Dunham, J.B., A.E. Rosenberger, C.H.. Luce, and B.E. Rieman. 2006. Influences of wildfire and channel disturbance on spatial and temporal variation in stream temperature and the distribution of fish and amphibians, Ecosystems, submitted.

Dwire, K. A. and Kauffman, J. B. 2003. Fire and riparian ecosystems in landscapes of the western USA. Forest Ecology and Management **178**(1-2): 61-74. DOI. 10.1016/S0378–1127(03)00053-7.

Fausch K.D., C.E. Torgersen, C.V. Baxter, and H.W. Li, 2002. Landscapes to Riverscapes: Bridging the Gap between Research and Conservation of Stream Fishes. BioScience **52**(6): 483–498.

Gray, J. R. A. and Edington, J. M. 1969. Effect of woodland clearance on stream temperature. Journal of the Fisheries Research Board of Canada **26**(2): 399-403.

Hardy, J. P., Melloh, R., Koenig, G., Marks, D., Winstral, A., Pomeroy, J. W. and Link, T. 2004. Solar Radiation Transmission through conifer canopies. Agricultural and Forest Meteorology **126**: 257-270. DOI: 10.1016/j.agrformet.2004.06.012.

Hatten, J. R. and Conrad, R. H. 1995. A comparison of summer stream temperatures in unmanaged and managed sub-basins of Washington's western Olympic peninsula. Northwest Indian Fisheries Commission, Olympia, WA.

Hewitt, M. J. 1990. Synoptic inventory of riparian ecosystems: the utility of Landsat Thematic Mapper data. Forest Ecology and Management. **33/34**: 605-620.

Huguenin, R. L., Karaska, M. A., Van Blaricom, D. and Jensen J. R. 1997. Subpixel classification of Bald Cypress and Tupelo Gum trees in Thematic Mapper Imagery. Photogrammetric Engineering and remote Sensing **63**(6): 717-725.

Hutchinson, C. F. 1991. Use of satellite data for famine early warning in sub-Saharan Africa. International Journal of Remote Sensing **2**: 1405-1421.

Jensen, J. R. 1996. Introductory Digital Image Processing: A remote sensing perspective, 2nd Edition. NJ: Prentice-Hall.

Johnson, S. L. 2004. Factors influencing stream temperatures in small streams: substrate effects and a shading experiment. Canadian Journal of Fisheries and Aquatic Sciences **61**: 913-923. DOI: 10.1139/f04-040.

Johnson, S. L. and Jones, J. A. 2000. Stream temperature responses to forest harvest and debris flow in western cascades, Oregon. Canadian Journal of Fisheries and Aquatic Sciences **57**(suppl. 2): 30-39.

Keleher C.J., Rahel F.J. 1996. Thermal limits to salmonid distributions in the rocky mountain region and potential habitat loss due to global warming: A geographic information system (GIS) approach, Transactions of the American Fisheries Society, **125** (1): 1-13.

Kriegler, F. J., Malila, W. A., Nalepka, R. F. and Richardson, W. 1969. Preprocessing transformations and their effect on multispectral recognition. Proceedings of the Sixth International Symposium on Remote Sensing of Environment. University of Michigan: 97-131.

Lawrence, R. L. and Ripple, W. J. 1998. Comparisons among vegetation indices and bandwise regression in a highly disturbed, heterogeneous landscape: Mount St. Helens, Washington. Remote Sensing of Environment **64**: 91-102. DOI:10.1016/S0034-4257(97)00171-5.

Malingreau, J. P. 1986. Global vegetation dynamics: satellite observations over Asia. International Journal of Remote Sensing **7**: 1121-1146.

Mason, J. 1983. Effects of topographic shading on the energy budget of small lakes.

Meyer, G. A. and Pierce, J. L., 2003. Climatic controls in fire-induced sediment pulses in Yellowstone National Park and Central Idaho: A long term perspective. Forest Ecology and Management, **178**(1-2)**:** 89-104. DOI. 10.1016/S0378–1127(03)00055-0.

Miller, D., Luce, C. H. and Benda L., 2003. Time, space and episodicity of physical disturbance in streams. Forest Ecology and Management, **178**(1-2): 121-140. DOI. 10.1016/S0378–1127(03)00057-4.

Minshall, G.W., and C.T. Robinson. 1993. Effects of the 1988 wildfires on stream systems of Yellowstone National Park: five-year comparison. University of Wyoming/National Park Service Research Center.

Minshall, G. W., Robinson, C. T., Lawrence, D. E. 1997. Postfires responses to lotic ecosystems in Yellowstone National Park, U.S.A. Canadian Journal of Fisheries and Aquatic Sciences, **54**: 2509-2525.

Moore, R.D.., P. Sutherland, T. Gomi, and A. Dhakal. 2005. Thermal Regime of Headwater Stream within a clear-cut, Coastal British Columbia, Canada. Hydrological Processes, 19, 2591-2608.

Morgan, P., Bunting, S. C., Black, A. E., Merrill, T., Barrett, S. 1996. Fire Regimes in the Interior Columbia River Basin: Past and Present. Dept. of Forest Resources, University of Idaho, Moscow, ID; Dept. of Range Resources, University of Idaho, Moscow, ID; Systems for Environmental Management, Kallispell, Montana, Missoula Montana. 32 pp.

Narumalani, S., Zhou, Y., Jensen, J. R. 1997. Application of remote sensing and geographic information systems to the delineation and anaylisi of riparian buffer zones. Aquatic Botany, **58**(3-4): 393-409. DOI: 10.1016/S0304-3770(97)00048-X

Poole, G. C. and Berman, C. H., 2001. An ecological perspective on in-stream temperature: Natural heat dynamics and mechanisms of human-caused thermal degradation. Environmental Management, **27**(6)**:**787-802. DOI: 10.1007/s002670010188.

Quinn, J. M. and McFarlane, P. N. 1989. Epilithon and dissolved oxygen depletion in the Manawatu River, New Zealand: simple models and management implications. Water Research **23**: 825-832.

Rich, P. M., Clark, D. B., Clark, D. A. and Oberbauer, S. F., 1993. Long term study of solar radiation regimes in a tropical wet forest using quantum sensors and hemispherical photography. Agricultural and Forest Meteorology, **65**: 107-127. DOI:10.1016/0168-1923(93)90040-O.

Robinson, S. A. and McCarthy, B. C. 1999. Potential factors affecting the estimation of light availability using hemispherical photography in oak forest understories. Journal of the Torrey Botanical Society **126**(4): 344-349.

Rouse, J. W., Haas, R. H., Schell, J. A. and Deering, D. W. 1973. Monitoring vegetation systems in the great plains with ERTS. Third ERTS Symposium, NASA SP-351 **vol 1**: 309-317.

Rutherford, J. C., Blackett, S., Blackett, C., Saito, L. and Davies Colley, R. 1997. Predicting the effects of shade on water temperature. New Zealand Journal of Marine and Freshwater Research **31**: 707-721.

Sinokrot, B. A. and Stefan, H. G. 1993. Stream temperature dynamics: measurements and modeling. Water Resources Research **29**: 2299-2312.

Smith, J. A., Lie Lin, T. and Ranson, K. J. 1980. The Lambertian Assumption and Landsat Data. Photogrammetric Engineering and Remote Sensing **46**:1183-1189.

Sugimoto, S., Nakamura, F. and Ito, A. 1997. Heat budget and statistical analysis of the relationship between stream temperature and riparian forest in the Toikanbetsu River basin, northern Japan. Journal of Forest Research **2**: 103-107.

Vannote, R. L., Minshall, G.W., Cummins, K. M., Sedell, J. R. and Cushing, C. 1980. The river continuum concept. Canadian Journal of Fisheries and Aquatic Sciences, **37**: 130-137.

Webb, B.W. and Y. Zhang. 1997. Spatial and seasonal variability in the components of the river heat budget. Hydrological. Processes. **11**:79-101.

Webb, B. W. and Zhang, Y. 1999. Water temperatures and heat budgets in Dorset chalk water courses. Hydrological Processes **13**(3): 309-421. DOI: 10.1002/(SICI)1099-1085(19990228)13:3<309::AID-HYP740>3.0.CO;2-7

Weiss, S. B., Rich, P. M., Murphy, D. D., Calvert, W. H., Ehlrich, P. R., 1991. Forest canopy structure at overwintering Monarch butterfly sites: measurements with hemispherical photography. Conservation Biology, **5**: 165-175.

White, J. D., Running, S. W., Nemani, R., Keene, R. E. and Ryan, K. C. 1997. Measurements and remote sensing of LAI in Rocky Mountain montane ecosystems. Canadian Journal of Forest Research **27**: 1714-1727.

Wiegand, C. L., Maas, S. J., Aase, J. K., Hatfield, J. L., Pinter, P. J., Jackson, R. D., Kanemasu, E. T. and Lapitan, R. L. 1992. Multisite analyses of spectral-biophysical data for wheat. Remote Sensing of Environment **42**: 1-21. DOI:10.1016/0034-4257(92)90064-Q

Williamson, H. D. 1994. Estimating sub-pixel components of a semi-arid woodland. International Journal of Remote Sensing **15**(16)**:** 3303-3307.

Wolter, P., Mladenoff, D., Host, G., Crow, T. 1995. Improved forest classification in the northern Lake States using multi-temporal Landsat Imagery. Photogrametric Engineering and Remote Sensing **61**(9): 1129-1143.

Xu, B, Gong, P. and Pu, R. 2003. Crown closure estimation of oak savannah in a dry season with Landsat TM imagery: comparison of various indices through correlation analysis. International Journal of Remote Sensing **24**(9): 1811-1822. DOI: 10.1080/01431160210144598.

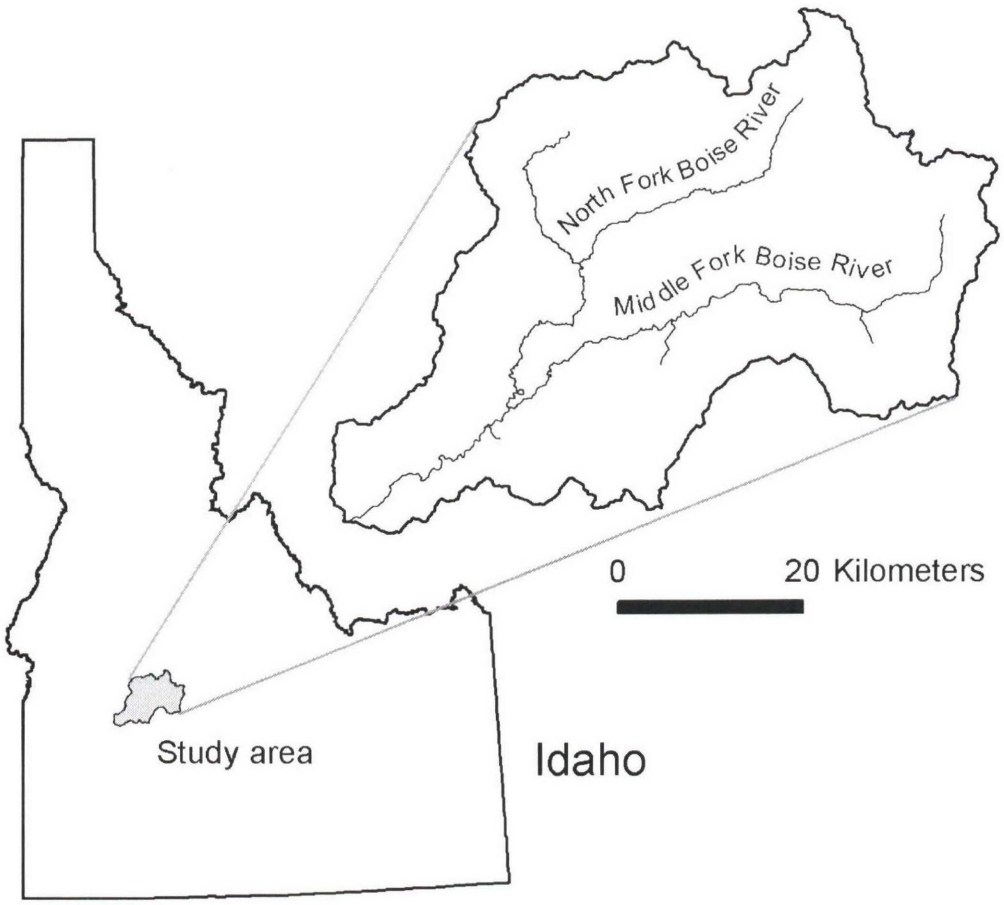

Figure 1: Location of study area in Idaho.

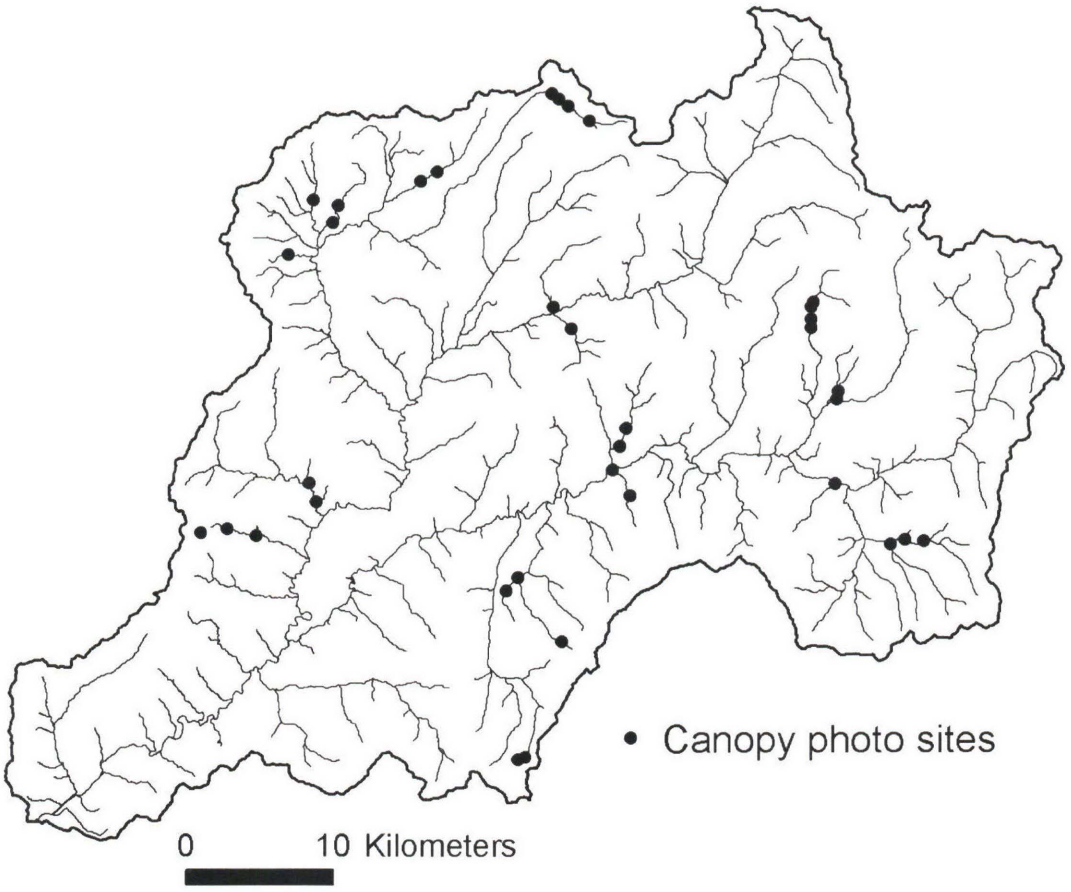

Figure 2: Map of the basin under study with the sites where hemispherical photographs were taken. Every point represents one location where 5 photos were taken.

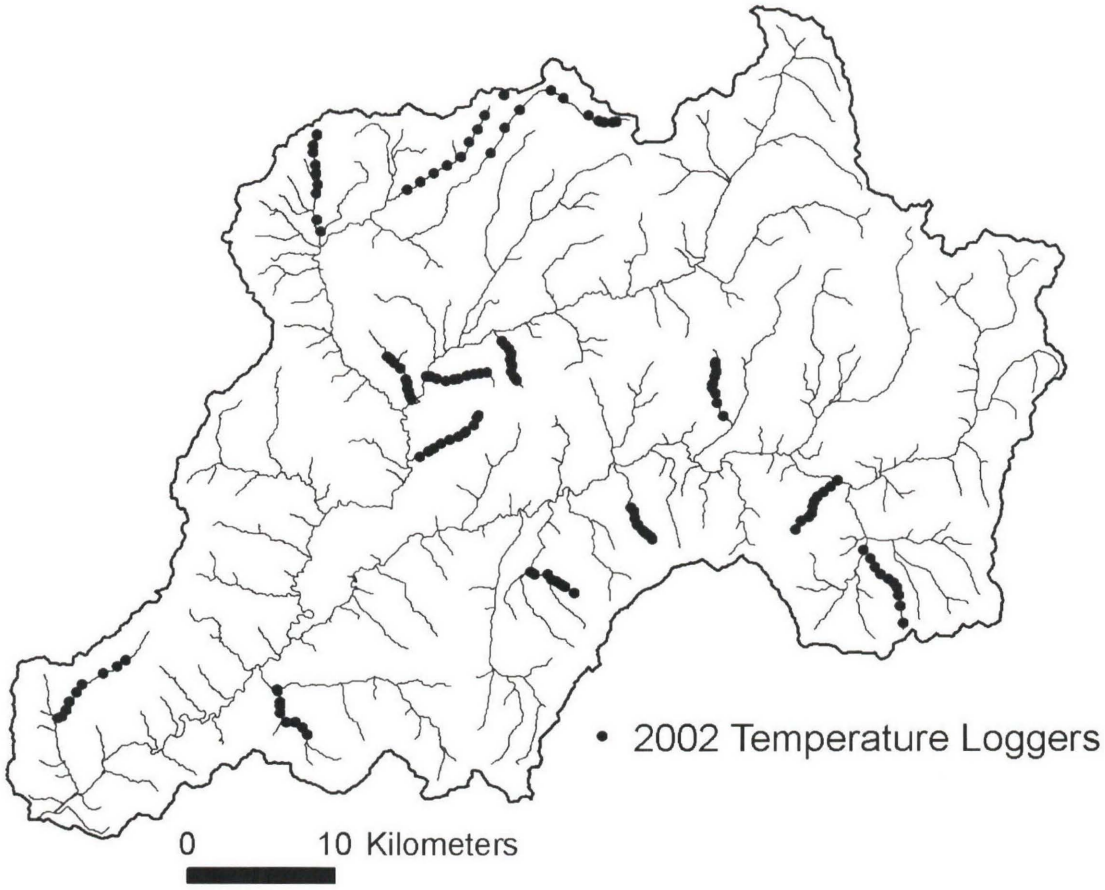

Figure 3: Map of the basin under study including the points where temperature loggers where placed in year 2002.

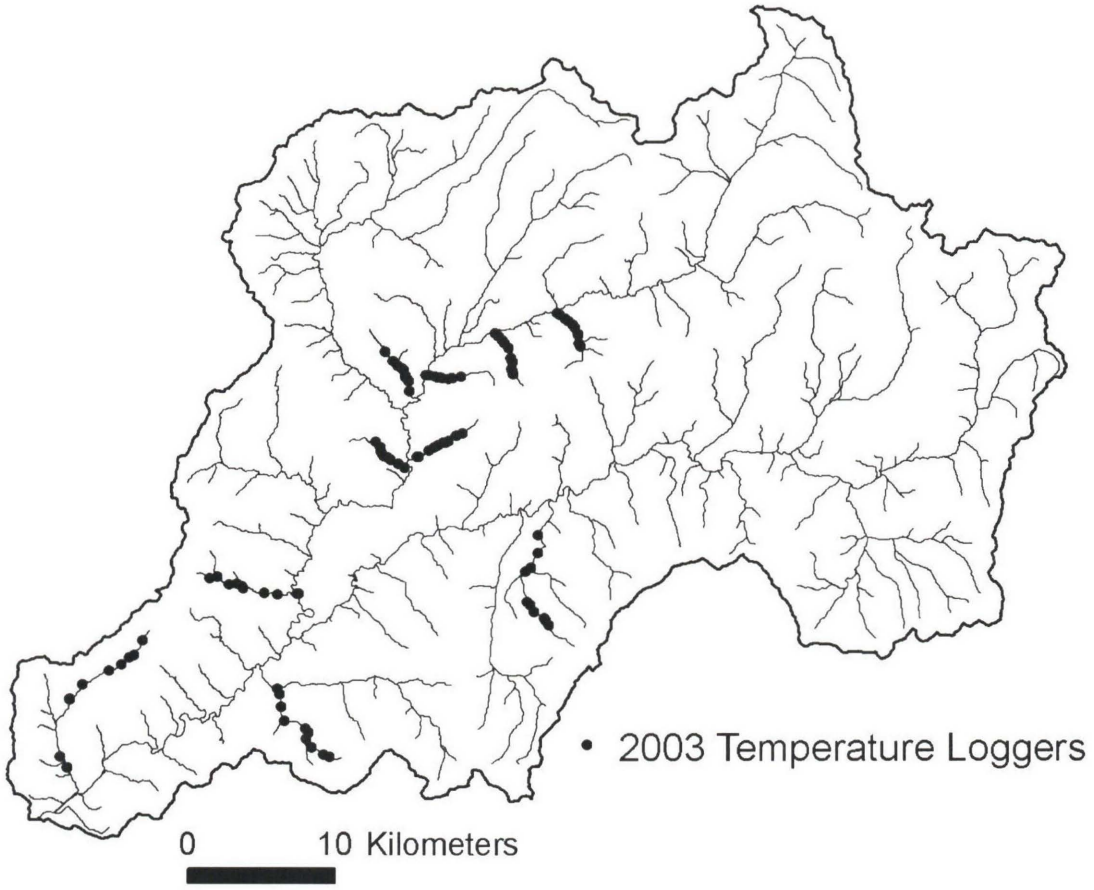

Figure 4: Map of the basin under study including the points where temperature loggers where placed in year 2003.

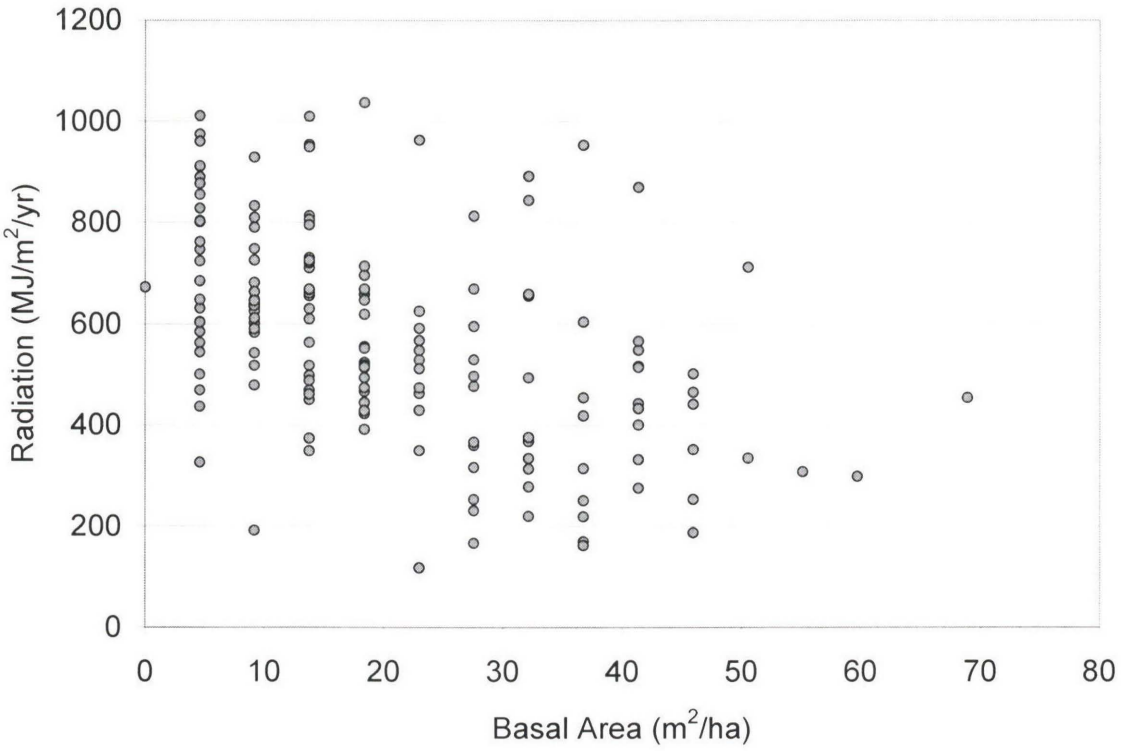

Figure 5: Relationship between the radiation values (MJ/m^2yr) obtained with the hemispherical photographs and the stand basal area (index of vegetation density) (m^2/Ha).

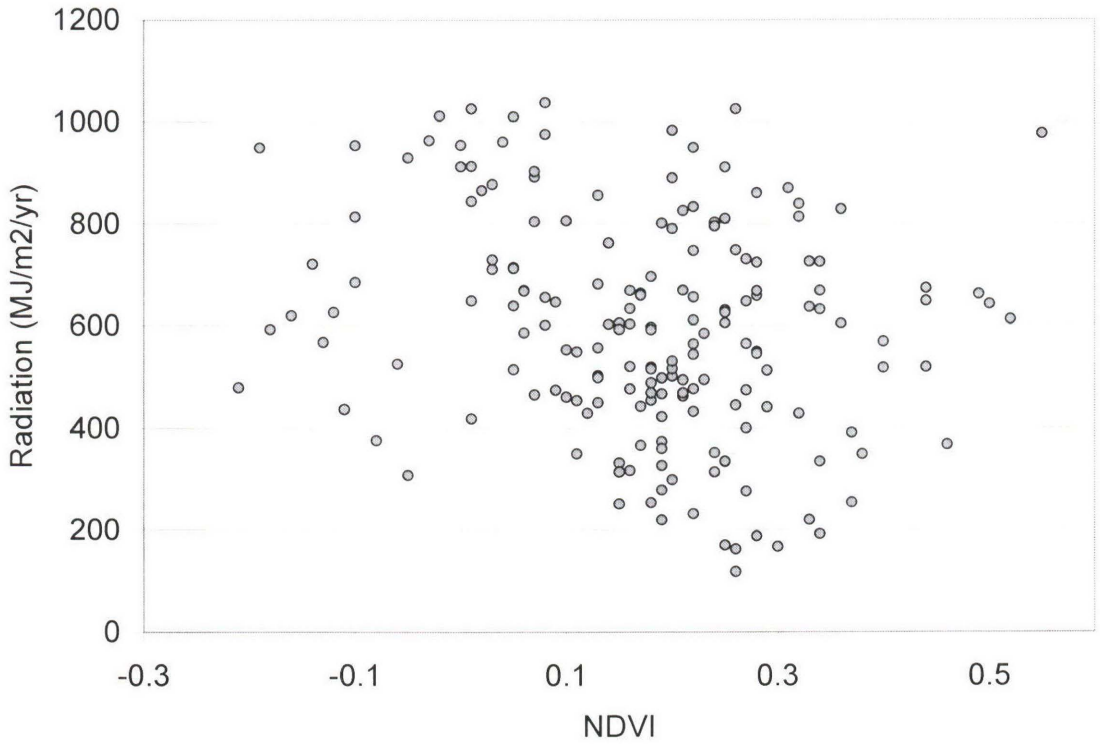

Figure 6: Relationship between the radiation values (MJ/m^2yr) obtained with the hemispherical photographs and the NDVI index.

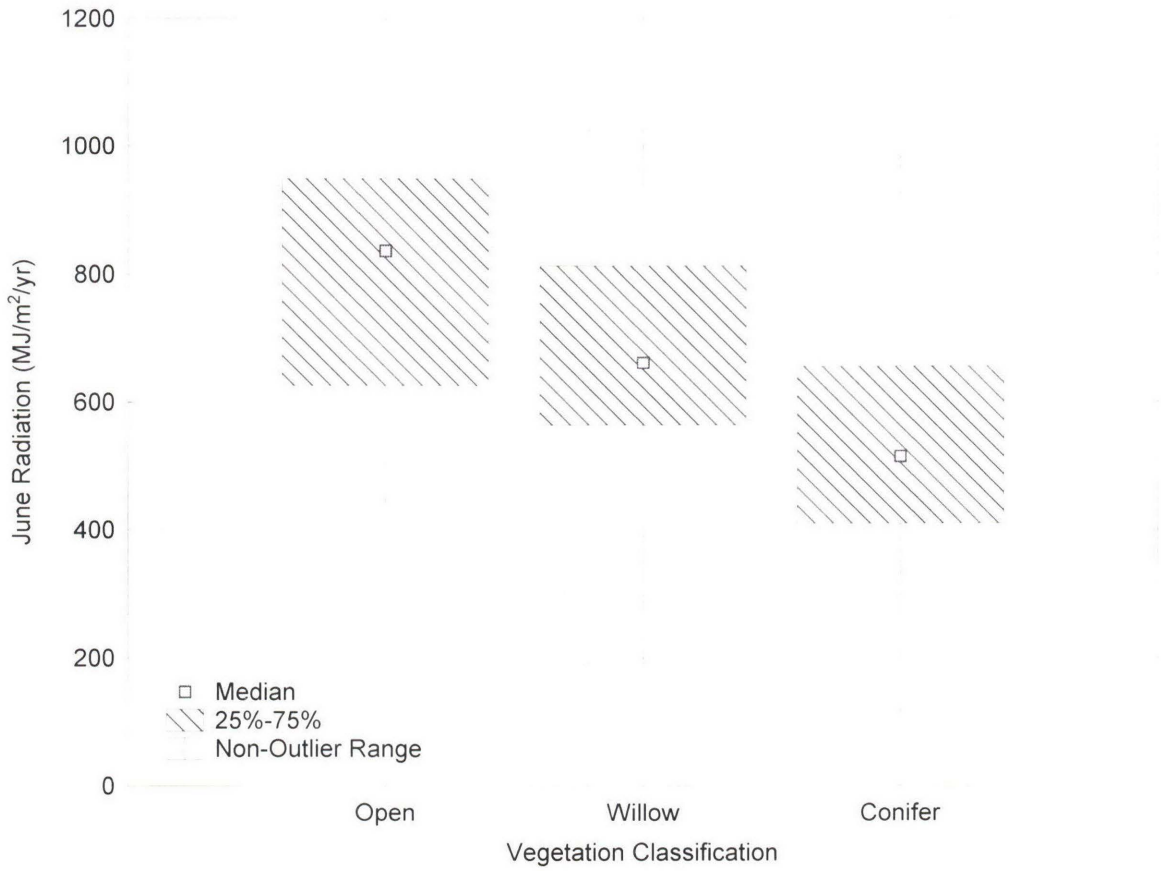

Figure 7: Box and Whisker plot for the relationships between the radiation (MJ/m^2yr) obtained through the hemispherical photographs and the three cover types into which each site was classified.

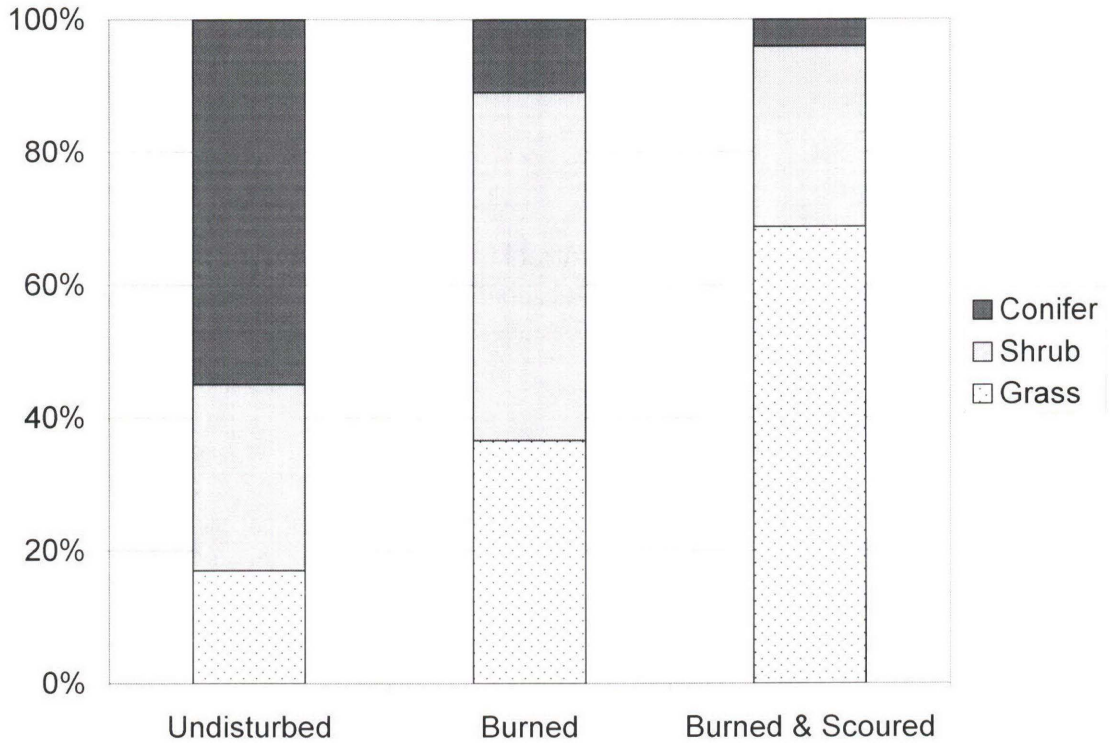

Figure 8: Fraction of pixels classed as conifer, shrub, or grass/open in segments of varying disturbance class.

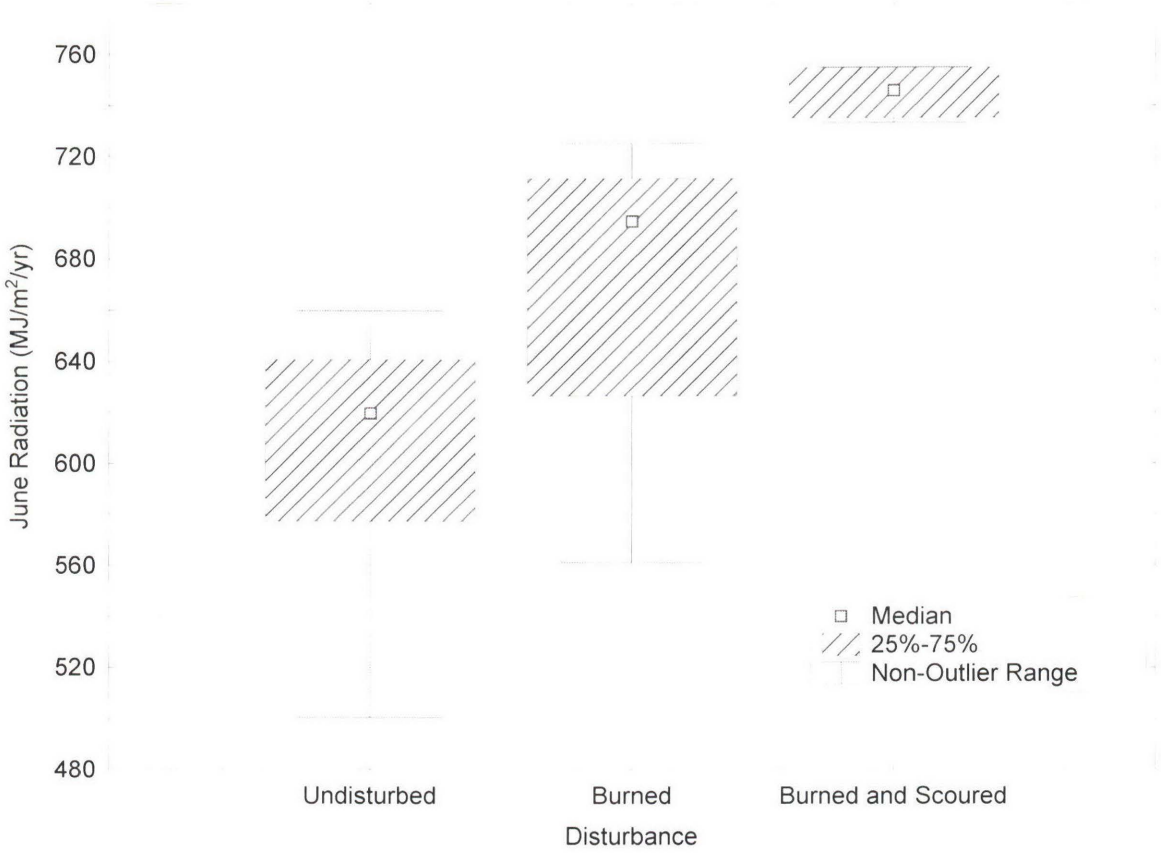

Figure 9: Box and Whisker plot for the relationships between the radiation (MJ/m^2yr) estimated from satellite image processing and the three disturbance classes into which each stream sampled in 2002 and 2003 were classified.

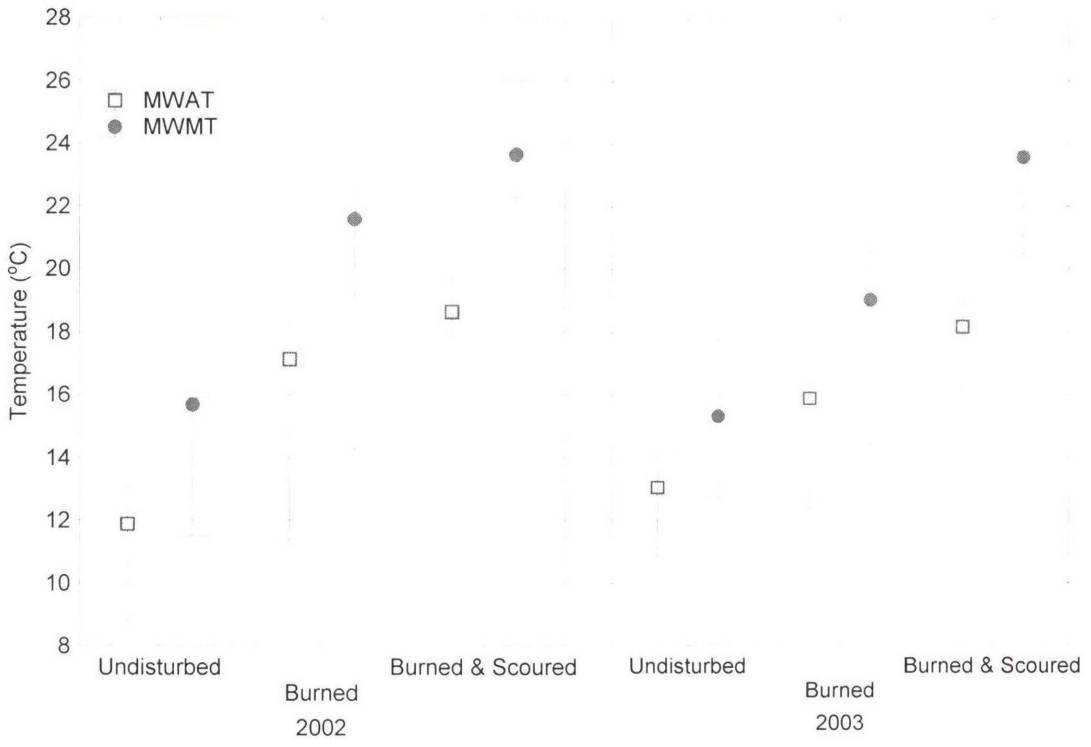

Figure 10: Whisker plot of medians, maximums, and mimimums for the relationships between the MWAT or MWMT (°C) and the three disturbance classes into which each stream sampled in 2002 and 2003 was classified. See Table 3 for ANOVA statistics.

A)

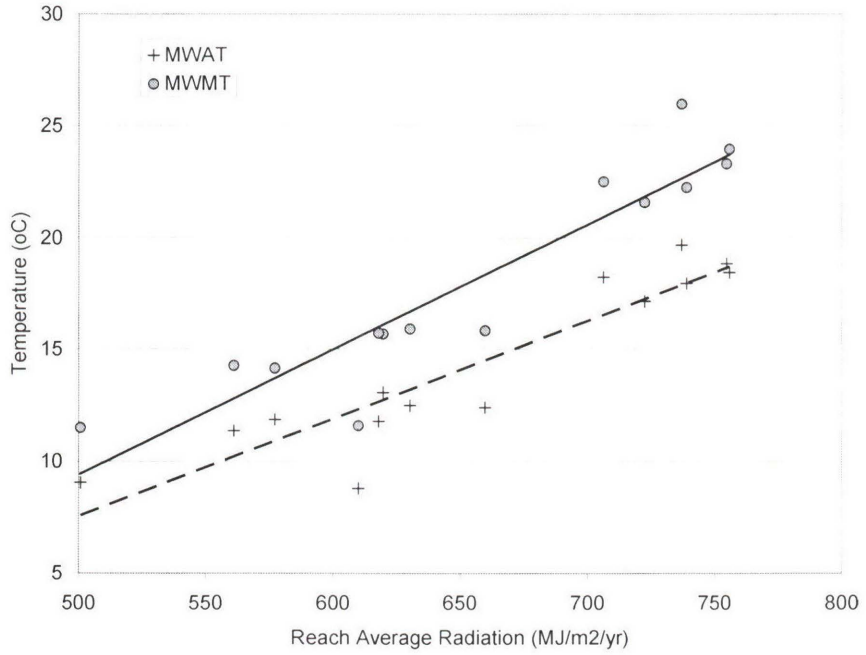

B)

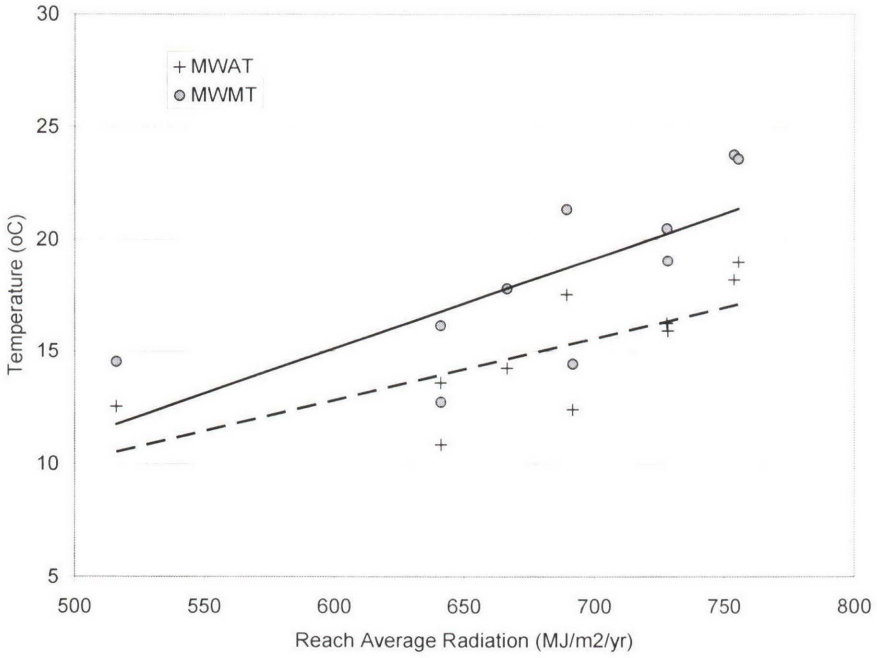

Figure 11: Regression models for the relationship between reach average radiation ($MJ/m^2/yr$) estimated from classified vegetation and MWAT and MWMT for each stream sampled in A) 2002 and B) 2003. See Table 4 for fit statistics.

Table 1: Classification accuracy for vegetation classification. All numbers in the table add to 100%. Open vegetation had a 48% chance of being classified otherwise, and Willow had a 43% chance of misclassification; while Conifers were only misclassified only 9% of the time. Vegetation classed as open has a high likelihood of being open (88%), while vegetation classed as willow is something else 40% of the time, and vegetation classed as conifer is open or willow 24% of the time.

	Classified Vegetation		
Observed Vegetation	Open	Willow	Conifer
Open	14%	2%	11%
Willow	1%	9%	6%
Conifer	1%	4%	52%

Table 2. Streams sampled in 2002 and 2003 in the Boise River basin (Figures 3 and 4) with the stream averaged MWAT obtained for each year in each stream and the average altitude of the sites. Each stream also classified according to disturbance classes.

Stream	Disturbance Class	Altitude (m) 2002	Altitude (m) 2003	Temp (°C) 2002	Temp (°C) 2003
Beaver C._1	Unburned	1651		13.09	
Beaver C._2	Unburned	1483	1401	12.51	9.92
Cottonwood C.	Burned	1396	1428	18.23	15.24
Crooked C.	Unburned	2039		19.05	
James C.	Unburned	1840		11.88	
French C.	Unburned		1375		11.89
Hungarian C.	Burned		1388		11.19
Little Rattle Snake C.	Burned and Reorganized	1339		19.68	
Lost C.	Burned	1507	1533	17.14	13.90
Lost Man C.	Unburned		1651		10.96
Phifer C.	Not burned	1856		8.80	
South Fork Sheep C.	Burned and Reorganized	1277	1397	17.94	14.26
Trail_1 C.(east)	Unburned	1654		11.80	
Trail_2 C.	Burned	1991		11.38	
Trail_3 C.	Unburned		1528		12.59
Trapper C.	Burned and Reorganized	1544	1511	18.43	15.99
West Warrior C.	Burned	1776		12.42	
Wren C.	Burned and Reorganized	1549	1513	18.83	17.07

Table 3: ANOVA results of the stream disturbance class versus both MWAT and MWMT (°C) for the streams sampled in summers 2002 and 2003. Whisker plots are shown in figure 9.

Year	Dependent Variable	Degrees of Freedom	F	p	R^2
2002	MWAT	2,11	16.9	0.0004	0.76
	MWMT	2,11	18.2	0.0003	0.77
2003	MWAT	2,7	6.2	0.03	0.64
	MWMT	2,7	7.0	0.02	0.67

Table 4. Regression results of estimated radiation values (MJ/m^2yr) versus both MWAT and MWMT (°C) obtained for the streams sampled in summers 2002 and 2003. Regression plots are shown in Figures 10 and 11.

Year	N	Dependent Variable	R^2	F	p	Model
2002	14	MWAT	84.7	66.5	<0.0001	0.04351R – 14.199
		MWMT	86.0	73.5	<0.0001	0.05597R – 18.586
2003	10	MWAT	51.4	8.46	0.02	0.02735R – 3.573
		MWMT	54.1	9.4	0.02	0.04009R – 8.922